Determination of the thermal conductivity of nanowires based on the metal-insulator transition of VO2

Jose Ordonez-Miranda, Laurent Belliard

Journal of Applied Physics ARTICLE pubs.aip.org/aip/jap

Determination of the thermal conductivity of nanowires based on the metal–insulator transition of VO_2

Cite as: J. Appl. Phys. **137**, 025105 (2025); doi: 10.1063/5.0250479
Submitted: 25 November 2024 · Accepted: 24 December 2024 ·
Published Online: 10 January 2025

Jose Ordonez-Miranda[a] and Laurent Belliard

AFFILIATIONS

Sorbonne Université, CNRS, Institut des Nanosciences de Paris, INSP, F-75005 Paris, France

[a]**Author to whom correspondence should be addressed:** jose.ordonez@cnrs.fr

ABSTRACT

We develop the theoretical foundation to determine the thermal conductivity of a single nanowire by using the optical contrast of the metallic and insulating domains of a VO_2 nanowire excited with either a temperature difference or a laser beam. Considering the temperature dependence of the VO_2 thermal conductivity, the heat flux and the temperature profile along a VO_2 nanowire are obtained and used to derive explicit expressions for the position of the metal/insulator domain interface as a function of the thermal excitation. This relation determines the variations of the metallic and insulating domains' lengths, which can be employed to retrieve the thermal conductivity of a single nanowire bonded to a VO_2 one. Furthermore, the advantages and disadvantages of each thermal excitation are discussed along with the appearance of invariants driving the one-dimensional nonlinear heat conduction along VO_2 nanowires.

I. INTRODUCTION

Vanadium dioxide (VO_2) is one of the most studied phase-change materials due to its first-order metal–insulator transition (MIT) at a temperature ($T_0 = 69\,^{\circ}C$) close to room temperature. At low temperature ($T < T_0$), VO_2 exhibits a monoclinic structure, which transforms into a tetragonal one at high temperature ($T > T_0$). This structural variation of VO_2 generates a significant change of its thermal, optical, and electrical properties.[1–4] For instance, in the low-temperature insulating phase, VO_2 exhibits high emissivity (∼0.8) and low thermal conductivity (∼3.6 $Wm^{-1}K^{-1}$), while in its high-temperature metallic phase, it has low emissivity (∼0.2) and high thermal conductivity (∼6 $Wm^{-1}K^{-1}$).[5–8] Considering that the emissivity (thermal conductivity) drives the propagation of radiative (conductive) heat currents, the MIT of VO_2 provides an effective way to manipulate the heat transport. In fact, the temperature dependence of these VO_2 properties has been exploited to develop thermal diodes,[6,9] thermal transistors,[10–16] thermal memristors,[17–19] and thermal logic gates.[20] These thermal devices aim to process information via phonons, electrons, and photons similar to their electronic counterparts.

The fascinating temperature dependence of the VO_2 physical properties has opened many avenues of research under the form of thin films mainly. However, with the synthesis of VO_2 nanowires[21] capable of supporting the one-dimensional (1D) propagation of electric and thermal currents, new applications start to emerge. By cantilevering a VO_2 nanowire from a silicon substrate and illuminating it with a laser beam of a stationary intensity, Cheng *et al.*[22] generated metallic and insulating domains along the nanowire. Considering that the metal/insulator domain interface is at temperature T_0, these latter authors moved its position by varying the laser beam intensity. The sharp optical contrast of the metallic and insulating phases was then used to experimentally determine the curve (interface position) vs (beam intensity), which allowed them to determine the local temperature, optical absorption, thermal conductivity, and interface thermal resistance of the VO_2 nanowire by fitting a suitable model. This optical and contactless technique, thus, capitalizes on the free motion of the metal/insulator domain interface and can be used to determine the thermal conductivity of a sample nanowire in contact with a VO_2 one.[22] Even though a freestanding VO_2 nanowire supported at one end only is nearly free of strain accumulation, its fabrication in thermal contact with a

sample nanowire could be challenging. Considering that the fabrication of supported VO_2 nanowires is relatively simple,[23] the extension of Cheng *et al.*[22] methodology for VO_2 nanowires supported at both ends is desirable but has not been developed yet.

In this work, we develop a theoretical methodology to determine the thermal conductivity of a single nanowire based on the optical contrast of the metallic and insulating domains of a supported VO_2 nanowire. This is done by deriving explicit expressions for the 1D heat flux and the temperature profile along a VO_2 nanowire excited with either a temperature difference or a laser beam of fixed intensity. For each configuration, we obtain analytical formulas for the position of the metal/insulator domain interface as a function of the thermal excitation and explain how they can be used to determine the thermal conductivity of a nanowire in thermal contact with a VO_2 one. The advantage and disadvantages of each configuration are also discussed along with the presence of invariants driving the nonlinear heat conduction in VO_2 nanowires.

II. THEORETICAL METHODOLOGY

Let us consider a VO_2 nanowire in thermal equilibrium with two thermal baths set at temperatures T_h and T_c, as shown in Fig. 1 (a). To generate heat current driven by the VO_2 MIT and the temperature difference $T_h - T_c > 0$, these temperatures are set around the VO_2 transition temperature $T_0 = 69\,^\circ\mathrm{C}$ ($T_c < T_0 < T_h$). The hot metallic portion of the nanowire will, thus, have length l_m and temperature $T > T_0$, while its cold insulating portion will exhibit length $l_i = l - l_m$ and temperature $T < T_0$. To find the spatial temperature profile $T(x)$ and lengths l_m and l_i, we assume that the system is placed in a vacuum chamber, and its maximum temperature is low enough ($T_h < 100\,^\circ\mathrm{C}$) to neglect the heat losses by heat convection and thermal radiation. Under this condition, the one-dimensional steady-state heat conduction along the nanowire is determined by Fourier's law,

$$q = -\kappa(T)\frac{dT}{dx}, \tag{1}$$

where q is the heat flux along the VO_2 nanowire with thermal conductivity κ. Considering that κ varies between its insulating ($\kappa_i = 3.6\,\mathrm{Wm^{-1}K^{-1}}$) and metallic ($\kappa_m = 6\,\mathrm{Wm^{-1}K^{-1}}$) values,[5] the temperature evolution of the VO_2 thermal conductivity is well described by[6]

$$\kappa(T) = \kappa_i + \frac{\kappa_m - \kappa_i}{1 + e^{-\gamma(T-T_0)}}, \tag{2}$$

where $T_0 = 342.5\,\mathrm{K}$ is the transition temperature and $\gamma = 1.6\,\mathrm{K^{-1}}$ is the phase-transition slope of $\kappa(T)$ at $T = T_0$. The values of κ_i, κ_m, T_0, and γ were determined by fitting Eq. (2) to the experimental data shown in Fig. 2.

For the considered steady-state heat conduction, the principle of energy conservation establishes that the heat flux q is constant and therefore, the integration of Eq. (1) for the VO_2 thermal conductivity in Eq. (3) yields the following expression for the temperature profile:

$$T(x) - T_0 + \frac{1}{\gamma\lambda}\ln[1 + Z(T(x))] = C - \frac{q}{\kappa_m}x, \tag{3}$$

where C is an integration constant, $\lambda = \kappa_m/(\kappa_m - \kappa_i)$, and $Z(T) = \exp[-\gamma(T - T_0)]$. The evaluation of Eq. (3) at the temperatures $T(x = 0)$ and $T(x = l)$ determines both q and C, which

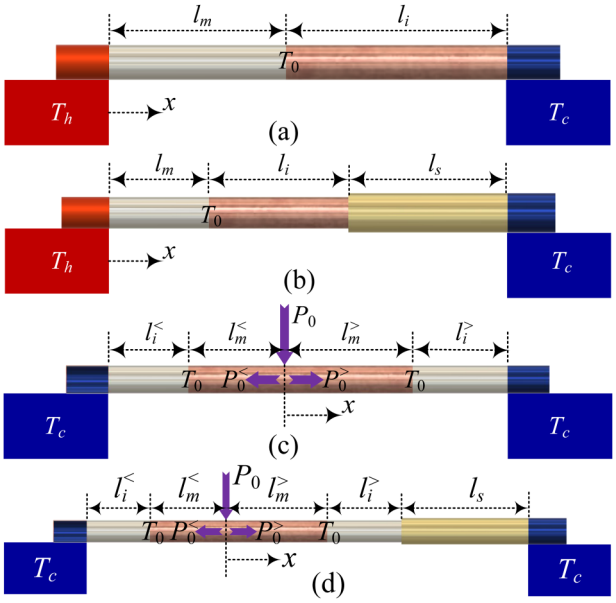

FIG. 1. Scheme of a VO_2 nanowire supporting the propagation of heat due to the (a) and (b) temperature difference $T_h - T_c > 0$ and (c) and (d) laser beam of power P_0. In (b) and (d), the VO_2 nanowire is in contact with another nanowire of length l_s.

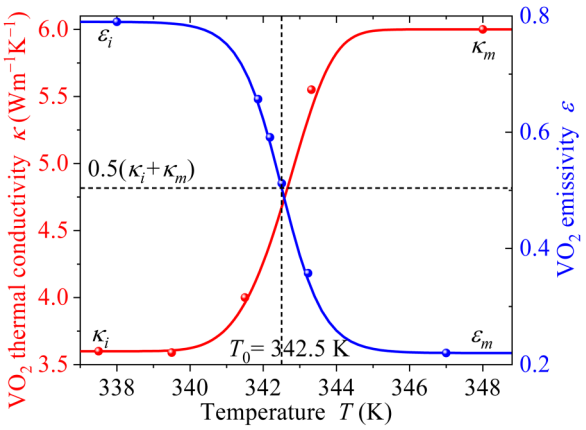

FIG. 2. Thermal conductivity and mean emissivity of VO_2 as functions of temperature. Dots stand for experimental data,[5,6] while lines represent the best fits predicted by Eq. (2) for the thermal conductivity.

allows expressing the heat flux and temperature profile as follows:

$$q = \frac{\kappa_m - \kappa_i}{\gamma l} \ln\left[\frac{f(T(0))}{f(T(l))}\right], \tag{4a}$$

$$f(T(x)) = [f(T(0))]^{1-x/l}[f(T(l))]^{x/l}, \tag{4b}$$

where $f(T) = [1 + Z(T)]/[Z(T)]^{\lambda}$ and $l = l_m + l_i$ is the total length of the VO_2 nanowire. Equations (4a) and (4b) will now be used to study the heat conduction along the four configurations shown in Fig. 1.

A. Temperature excitation of a VO_2 nanowire

This configuration consists of a single VO_2 nanowire supporting the 1D heat conduction due to the temperature difference $T_h - T_c > 0$ of its thermal baths, as shown in Fig. 1(a). These free-standing VO_2 nanowires can be grown by thermal evaporation before placing its ends on a substrate.[24] Considering that the interface thermal resistance of the VO_2 nanowire with the hot and cold thermal baths are, respectively, R_h and R_c, the temperatures $T(0)$ and $T(l)$ are determined by the boundary conditions $T_h - T(0) = R_h P$ and $T(l) - T_c = R_c P$, with $P = Aq$ and A being the heat power and cross-sectional area of the nanowire. Under these conditions, Eqs. (4a) and (4b) take the form

$$P = A\frac{\kappa_m - \kappa_i}{\gamma l} \ln\left[\frac{f(T_h - R_h P)}{f(T_c + R_c P)}\right], \tag{5a}$$

$$f(T(x)) = [f(T_h - R_h P)]^{1-x/l}[f(T_c + R_c P)]^{x/l}. \tag{5b}$$

Equations (5a) and (5b), thus, show that P and T have a strong nonlinear dependence on the temperatures T_h and T_c and position x such that $P = 0$ for $T_h = T_c$, as expected. To better understand the predictions of Eqs. (5a) and (5b), we consider the following limiting cases of $f(T) = \{1 + \exp[-\gamma(T - T_0)]\}\exp[\lambda\gamma(T - T_0)]$:

$$f(T) \approx \begin{cases} e^{\lambda\gamma(T-T_0)} & \text{for} \quad T \gg T_0, \\ e^{\gamma(1-\lambda)(T_0-T)} & \text{for} \quad T \ll T_0. \end{cases} \tag{6}$$

Considering that the excitation temperatures T_h and T_c are, respectively, high and low enough to ensure the condition $T_c + R_c P \ll T_0 \ll T_h - R_h P$, the application of Eq. (6) to simplify Eq. (5a) yields the following heat: power

$$P = \frac{\kappa_m(T_h - T_0) + \kappa_i(T_0 - T_c)}{l/A + \kappa_m R_h + \kappa_i R_c}, \tag{7}$$

which reduces to the typical model of thermal resistances in series for $k_m = k_i$. Equation (7), thus, takes into account the temperature variation ($\kappa_m > \kappa_i$) of the VO_2 thermal conductivity and shows that the contribution of the metallic and insulating phases is weighted by their corresponding thermal conductivities. According to Fig. 1(a), the length l_m of the VO_2 nanowire in the metallic phase is given by $T(x = l_m) = T_0$, for which $f(T) = 2$. Under this condition and the assumption of low and high enough temperatures ($T_c + R_c P \ll T_0 \ll T_h - R_h P$), the combination of Eqs. (5b) and (6) yields

$$\frac{l_m}{l} = \frac{a_1(T_h - T_0) - a_2}{T_h - T_0 + a_3}, \tag{8}$$

where the coefficients a_n for $n = 1, 2, 3$ are given by

$$a_1 = 1 + \frac{R_c}{R_i}, \tag{9a}$$

$$a_2 = \left(a_1 + \frac{R_h}{R_m}\right)\left(1 - \frac{\kappa_i}{\kappa_m}\right)\frac{\ln(2)}{\gamma} + \frac{R_h}{R_i}(T_0 - T_c), \tag{9b}$$

$$a_3 = \frac{\kappa_i}{\kappa_m}(T_0 - T_c), \tag{9c}$$

where $R_m = l/(A\kappa_m)$ and $R_i = l/(A\kappa_i)$ are the thermal resistances of the VO_2 nanowire in its metallic and insulating phases, respectively. Equation (8) indicates that the nonlinear increase of l_m with $\Delta T_h = T_h - T_0$ can be used to determine the parameters a_1, a_2, and a_3 and, therefore, to retrieve the interface thermal resistances R_h and R_c as well as the thermal conductivity contrast k_m/k_i, provided that the other parameters of the VO_2 thermal conductivity are known. Taking into account that the length l_m can be measured with an infrared thermal camera, its reading for different values of the excitation temperature T_h, provides a method to characterize the thermal contact of the VO_2 nanowire with its thermal baths.

B. Temperature excitation of a sample nanowire

This configuration consists of a VO_2 nanowire bonded to a sample (other than VO_2) nanowire of length l_s, cross-sectional area A_s, and thermal conductivity k_s, as shown in Fig. 1(b). A single suspended nanowire can be synthesized by anisotropic etching and thermal oxidation before being bonded to a VO_2 nanowire using microprobes, as done in previous works.[22,25–29] As the VO_2 and sample nanowires are, respectively, in thermal contact with the hot and cold thermal baths, the heat power $P = Aq$ unidirectionally flows from the VO_2 nanowire to the sample one and is given by Eq. (4a). Assuming that k_s is nearly independent of temperature for temperatures between T_c and T_h, the principle of energy conservation establishes that P is also given by Fourier's law of heat conduction,

$$P = A_s k_s \frac{T_s(l) - T_s(l + l_s)}{l_s}, \tag{10}$$

where $T_s(x)$ is the temperature at position x along the sample nanowire. Considering that the thermal resistances at the interfaces VO_2/sample and sample/bath are, respectively, R and R_c, the boundary conditions $T(l) - T_s(l) = RP$ and $T_s(l + l_s) - T_c = R_c P$ combined with Eq. (10) establish that the lowest temperature of the VO_2 nanowire is given by $T(l) = T_c + (R + R_s + R_c)P$, with $R_s = l_s/(A_s k_s)$ being the thermal resistance of the sample nanowire. This latter relation for $T(l)$ together with the boundary condition $T_h - T(0) = R_h P$ at $x = 0$ determines the heat power P in Eq. (4a).

The final result is

$$P = A\frac{\kappa_m - \kappa_i}{\gamma l}\ln\left[\frac{f(T_h - R_h P)}{f(T_c + (R + R_s + R_c)P)}\right]. \tag{11}$$

The heat power, thus, exhibits a nonlinear dependence on the temperatures T_h and T_c such that $P = 0$ for $T_h = T_c$, as expected. For $T_h > T_c$, on the other hand, the application of Eq. (6) for the high $(T_h - R_h P \gg T_0)$ and low $(T_c + (R + R_s + R_c)P \ll T_0)$ temperature approximations of Eq. (11) provides the following analytical solution for the heat power:

$$P = \frac{\kappa_m(T_h - T_0) + \kappa_i(T_0 - T_c)}{l/A + \kappa_m R_h + \kappa_i(R + R_s + R_c)}. \tag{12}$$

Equation (12) explicitly shows that P is determined by the temperature variation $(\kappa_m > \kappa_i)$ of the VO_2 thermal conductivity and reduces to Eq. (7) in the absence of a sample nanowire $(R = 0 = R_s)$, as expected. Furthermore, considering that the spatial distribution $T(x)$ of the temperature along the VO_2 nanowire is determined by Eq. (4b), with $T(0)$ and $T(l)$ given just below Eq. (10), the length l_m of the VO_2 nanowire in the metallic phase is given by $T(x = l_m) = T_0$. Under this condition $f(T) = 2$, Eq. (4b) reduces to

$$f(T_h - R_h P)\exp\left[-\frac{\gamma l_m P}{A(k_m - k_i)}\right] = 2. \tag{13}$$

The combination of Eqs. (12) and (13), thus, predicts the following metallic length:

$$\frac{l_m}{l} = \frac{b_1(T_h - T_0) - b_2}{T_h - T_0 + a_3}, \tag{14}$$

where a_3 is given by Eq. (9c) and the other coefficients are defined by

$$b_1 = 1 + \frac{R + R_s + R_c}{R_i}, \tag{15a}$$

$$b_2 = \left(b_1 + \frac{R_h}{R_m}\right)\left(1 - \frac{\kappa_i}{\kappa_m}\right)\frac{\ln(2)}{\gamma} + \frac{R_h}{R_i}(T_0 - T_c). \tag{15b}$$

Equation (15), thus, indicates that the optical reading of l_m for different excitation temperatures T_h can be used to determine the total thermal resistance $R + R_s + R_c$ and, hence, the effective thermal conductivity $k_{\text{eff}} = l_s/[A_s(R + R_s + R_c)]$ of the sample nanowire through a fitting procedure. As the interface thermal resistances R and R_c can be much smaller than the sample thermal resistance $R_s = l_s/(A_s k_s)$, for a long enough sample nanowire, k_{eff} represents a good estimation of the actual thermal conductivity k_s. In contrast to other methodologies reported in the literature,[22,26] the proposed method does not require the measurement of the heat power or temperature of both thermal baths to determine k_{eff}.

C. Laser beam excitation of a VO_2 nanowire

In this configuration, a single VO_2 nanowire is placed between two thermal baths set at the same temperature T_c and is illuminated with a laser beam of power P_0, as shown in Fig. 1(c). The power $P_a = \alpha P$ absorbed by the VO_2 nanowire is determined by its absorbance α and the incident power P physically striking the nanowire. Considering that the laser beam spot has a Gaussian profile with radius R and intensity $I(r) = 2P_0/(\pi R^2)\exp\left[-2(r/R)^2\right]$ such that its center coincides with the axis of the VO_2 nanowire of diameter $2a$, as shown in Fig. 3(a), P is given by

$$\frac{P}{4} = \int_0^R \int_0^{x\tan(\theta)} I(x, y)dxdy + \int_0^{\theta}\int_0^R I(r)rdrd\theta', \tag{16}$$

where $r = \sqrt{x^2 + y^2}$ and $\sin(\theta) = a/R$. The integration of the integrals in Eq. (16) for the Gaussian profile I yields $P = \beta P_0$, with β being a geometrical factor given by

$$\beta = \frac{2}{\pi}\left(1 - e^{-2}\right)\arcsin(a/R) + 2\sqrt{\frac{2}{\pi}}\int_0^1 \text{erf}\left(\frac{\sqrt{2}\xi}{\sqrt{(R/a)^2 - 1}}\right)e^{-2\xi^2}d\xi, \tag{17}$$

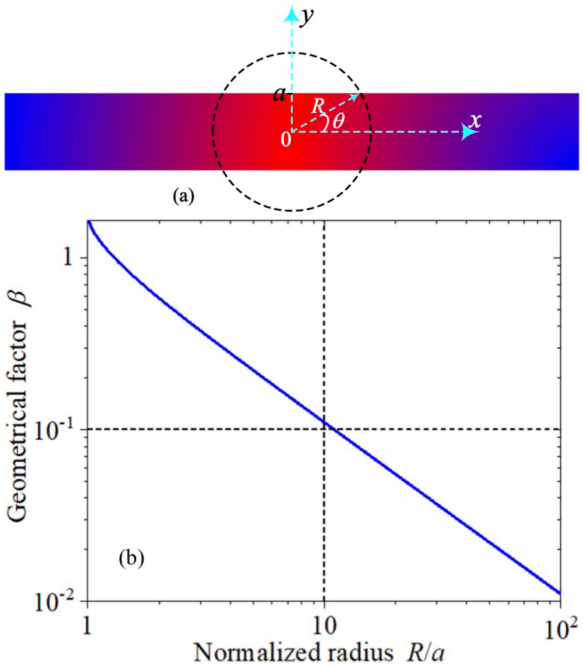

FIG. 3. (a) Schema of a laser beam spot of radius R and center along the axis of a nanowire of radius a. (b) Geometrical factor β as a function of the normalized radius R/a.

where erf(.) is the error function. β is, thus, fully determined by the ratio R/a and its value decreases when R/a increases, as shown in Fig. 3(b). Note that $\beta \sim a/R$ such that $\beta \approx 0.11$ for $R = 10a$. The fraction $\beta = P/P_0$ of the laser beam power striking the nanowire is, thus, roughly given by the ratio a/R of radii of the nanowire and the laser beam spot. The absorbed power is, therefore, correlated to the total incident power by

$$P_a = \alpha\beta P_0 = P_a^< + P_a^>, \tag{18}$$

where $P_a^<$ and $P_a^>$ are the respective powers flowing toward the left and right thermal baths, as shown in Fig. 1(c).

Considering that the interface thermal resistances of the VO_2 nanowire with the left and right thermal baths are, respectively, $R^<$ and $R^>$, the boundary conditions $T(-l) - T_c = R^< P_a^<$ and $T(l) - T_c = R^> P_a^>$ together with Eq. (4a) establish that the heat powers $P_a^<$ and $P_a^>$ are given by

$$P_a^< = A\frac{\kappa_m - \kappa_i}{\gamma l^<}\ln\left[\frac{f(T(0))}{f(T_c + R^< P_a^<)}\right], \tag{19a}$$

$$P_a^> = A\frac{\kappa_m - \kappa_i}{\gamma l^>}\ln\left[\frac{f(T(0))}{f(T_c + R^> P_a^>)}\right], \tag{19b}$$

where $l^<$ and $l^>$ are the nanowire lengths to the left and right of its heating central point at $x = 0$, as shown in Fig. 1(c). These lengths drive the absorbed powers through the relation $l^< P_a^< = l^> P_a^>$, in the absence of thermal resistances ($R^< = R^> = 0$) or when they fulfill the relation $R^< P_a^< = R^> P_a^>$, as established by Eqs. (19a) and (19b). The temperature $T(0)$ determining the values of $P_a^<$ and $P_a^>$ can be calculated from the temperature profile in Eq. (4b), as follows:

$$f(T) = \begin{cases} [f(T(0))]^{1+x/l^<}\left[f(T_c + R^< P_a^<)\right]^{-x/l^<}, & x < 0, \\ [f(T(0))]^{1-x/l^<}\left[f(T_c + R^> P_a^>)\right]^{x/l^<}, & x > 0. \end{cases} \tag{20}$$

The evaluation of Eq. (20) for the VO_2 transition temperature $T_0 = T(x = -l_m^<) = T(x = l_m^>)$ $(f(T_0) = 2)$ in combination with Eqs. (19a) and (19b) yields

$$l_m^< P_a^< = l_m^> P_a^> = A\frac{\kappa_m - \kappa_i}{\gamma}\ln\left(\frac{f(T(0))}{2}\right). \tag{21}$$

The product $l_m^{\lessgtr} P_a^{\lessgtr}$ between the VO_2 nanowire length in the metallic phase and the corresponding thermal power generating it are, thus, an invariant of heat conduction for a given temperature $T(0)$. By inserting Eq. (21) into Eqs. (19a) and (19b), one obtains

$$l_i^< P_a^< = A\frac{\kappa_m - \kappa_i}{\gamma}\ln\left[\frac{2}{f(T_c + R^< P_a^<)}\right], \tag{22a}$$

$$l_i^> P_a^> = A\frac{\kappa_m - \kappa_i}{\gamma}\ln\left[\frac{2}{f(T_c + R^> P_a^>)}\right], \tag{22b}$$

where $l_i^< = l^< - l_m^<$ and $l_i^> = l^> - l_m^>$ are the VO_2 nanowire lengths in the insulating phase at the left and right side of the heating point, respectively. Note that the product $l_i^{\lessgtr} P_a^{\lessgtr}$ becomes an invariant of heat conduction in the absence of the interface thermal resistances ($R^< = R^> = 0$). In the presence of theses resistances, on the other hand, the solutions of Eqs. (22a) and (22b) for the powers $P_a^<$ and $P_a^>$ can analytically be derived for $T_0 \ll T_c + R^< P_a^<$ and $T_0 \ll T_c + R^> P_a^>$. Under these two latter conditions, the application of Eq. (6) yields

$$P_a^<\left(\frac{l_i^<}{Ak_i} + R^<\right) = P_a^>\left(\frac{l_i^>}{Ak_i} + R^>\right) = T_0 - T_c + \left(\frac{\kappa_m}{\kappa_i} - 1\right)\frac{\ln(2)}{\gamma}. \tag{23}$$

Equation (23), thus, represents a second invariant of heat conduction that takes into account the impact of the interface thermal resistances. Interestingly, the combination of the first equalities of Eqs. (21) and (23) establishes that the insulating nanowire lengths $l_i^>$ and $l_i^<$ have the following linear correlation independent of the absorbed powers:

$$l_i^> = \frac{(l^>/Ak_i + R^>)l_i^< + R^< l^> - R^> l^<}{l^</Ak_i + R^<}. \tag{24}$$

The optical reading of the lengths $l_i^>$ and $l_i^<$ for different injected powers P_0 and their subsequent linear fitting via Eq. (24) determine its slope and intercept. The definition of these two parameters in Eq. (24) can then be used to retrieve the interface thermal resistances $R^<$ and $R^>$, provided that the insulating VO_2 thermal conductivity κ_i is known. In particular, note that a zero or nearly zero intercept would indicate that $R^<$ and $R^>$ are negligible (for $l^< \neq l^>$) or equal (for $l^< = l^>$). In any case, after determining the values of $R^<$ and $R^>$, the VO_2 nanowire absorbance α could also be measured through the following model resulting from the combination of Eqs. (18) and (23):

$$mP_0 = \frac{1}{l_i^</Ak_i + R^<} + \frac{1}{l_i^>/Ak_i + R^>}, \tag{25}$$

where $m = \alpha\beta[T_0 - T_c + (\kappa_m/\kappa_i - 1)\ln(2)/\gamma]^{-1}$. The same reading of $(l_i^<, l_i^>)$ for different values of P_0 that are used for determining $R^<$ and $R^>$ via Eq. (24) can, therefore, be used to determine m and, therefore, α via the fitting of Eq. (25).

D. Laser beam excitation of a sample nanowire

We here consider a VO_2 nanowire in thermal contact with a sample nanowire of length l_s, cross-sectional area A_s, and thermal conductivity k_s, as shown in Fig. 1(d). Unlike the nanowires excited with a temperature difference in Fig. 1(b), in the present configuration, the nanowires are excited with a laser beam injecting its power on the VO_2 nanowire. For this thermal excitation and the lengths' distribution shown in Fig. 1(d), the heat conduction along the nanowires is determined by Fourier's law $P_a^> = A_s k_s[T_s(l^>) - T_s(l^> + l_s)]/l_s$ and boundary conditions: $T(-l^<) - T_c = R^< P_a^<$, $T(l^>) - T_s(l^>) = RP_a^>$, and $T_s(l^> + l_s) - T_c = R^> P_a^>$, with $T(x)$ and $T_s(x)$ being the respective

temperatures along the VO_2 and sample nanowires with interface thermal resistance R, while $R^<$ and $R^>$ are the interface thermal resistances of the VO_2 and sample nanowires with their corresponding left and right thermal baths. These conditions determine $T(-l^<) = T_c + R^< P_a^<$ and $T(l^>) = T_c + P_a^>(R + R_s + R^>)$, which in combination with Eqs. (4a) and (4b) establish that absorbed powers and temperature distribution are, respectively, given by Eqs. (19) and (20), with $R^>$ replaced by $R + R_s + R^>$. Therefore, under this replacement, Eqs. (24) and (25) also apply for the present configuration and can be used to determine the total thermal resistance $R_T = R + R_s + R^>$ of the sample nanowire via a fitting procedure. For a long enough sample nanowire, its thermal resistance $R_s = l_s/(A_s k_s)$ can become much higher than the interface thermal resistances ($R_s \gg R$ and $R^>$), and therefore, $R_T \approx R_s$ could be used to determine the thermal conductivity of the sample nanowire.

III. RESULTS AND DISCUSSION

We now analyze the heat flux, the temperature profile, and lengths of the metallic and insulating domains of a VO_2 nanowire with and without thermal contact with a sample nanowire. Numerical calculations are done for the VO_2 thermal conductivity defined in Eq. (2) and shown in Fig. 2.

The heat flux q predicted by Eq. (4a) for a VO_2 nanowire supported by two thermal baths is shown in Fig. 4(a) as a function of the temperature T_h of the hotter thermal bath. For $T_h < T_0$, the VO_2 nanowire is in an insulating phase, and therefore, $q = \kappa_i(T_h - T_c)/l$ (blue dashed line) is driven by the corresponding thermal conductivity κ_i, as established by the Fourier law. This linear relation $q(T_h)$ changes to $ql = \kappa_i(T_0 - T_c) + \kappa_m(T_h - T_0)$ (red dashed line) when part of the VO_2 nanowire is in its metallic phase ($T_h > T_0$). This latter relation shows that q is simply determined by the sum of heat fluxes along the insulating and metallic domains of the VO_2 nanowire. The slope variation $(\kappa_m - \kappa_i)/l$ of the heat flux $q(T_h)$ through the VO_2 transition temperature $T_h = T_0$, thus, results from the thermal conductivity difference between the metallic and insulating phases of VO_2 and leads to a nonlinear spatial distribution of temperature T, as shown in Fig. 4(b). Note that T exhibits two linear regimes related to the two phases of VO_2. The slope change between these two regimes increases with T_h for values higher than T_0. The fact that q and T exhibit smooth transitions around the MIT of VO_2 indicates that the typical consideration of a VO_2 nanowire like the composition of two nanowires with temperature-independent thermal conductivities κ_i and κ_m is not accurate to describe the heat conduction along it.

Figure 5(a) shows the length l_m of the metallic zone of a VO_2 nanowire as a function of the hot thermal bath temperature T_h, for a VO_2 nanowire in thermal contact with a sample nanowire excited by two thermal baths [see Fig. 1(b)]. Note that l_m appears for $T_h > T_0$ and increases with T_h, as expected. This non-linear increase gets stronger for a higher thermal resistance $\rho = (R + R_s + R_c)/R_m$, as predicted by Eq. (14). This fact indicates that the VO_2 nanowire reaches its full metallic phase ($l_m = l$) at lower T_h values for a sample with higher thermal resistance $R_s = l_s/(A_s\kappa_s)$. Importantly, the significant variation of l_m with ρ establishes that the optical

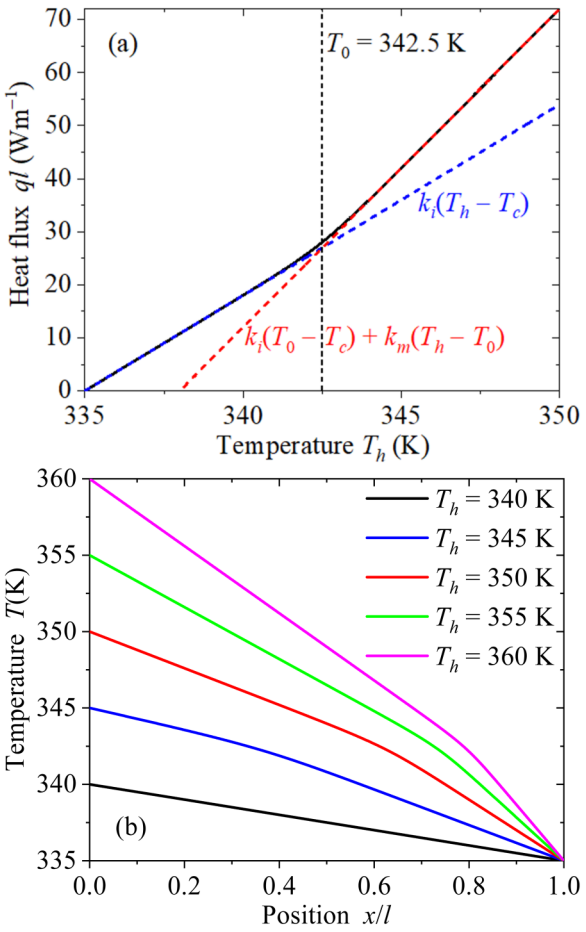

FIG. 4. (a) Heat flux and (b) temperature of a VO_2 nanowire as functions of the temperature $T(0) = T_h$ and position x/l, respectively. Calculations were done with Eqs. (4a) and (4b) and $T(l) = T_c = 335$ K.

recording of the curve l_m vs T_h could be used to accurately determine the total thermal resistance $R + R_s + R_c$ of the sample nanowire. On the other hand, when the thermal excitation provided by the temperature difference $T_h - T_c$ of the thermal baths is changed by a laser beam, the sensitivity of l_m (and, hence, $l_i^< = l^< - l_m^<$) to ρ significantly weakens, as shown by the dashed lines in Fig. 5(b). By contrast, the linear correlation of the insulating lengths $l_i^>$ and $l_i^<$ exhibits relatively higher sensitivity to ρ, and hence, it could be used to find $R + R_s + R_c$ by fitting Eq. (24). As Eq. (24) arises from the two 1D heat conduction invariants of VO_2 and is independent of the excitation source, this latter approach has the advantage of not involving the VO_2 absorbance and hence, it avoids the difficulty found in previous works[22,30] to accurately determine the absorbed power of the laser beam. The behavior and sensitivity of the curves $l_m(T_h)$ and $l_i^>(l_i^<)$ shown in Figs. 5(a) and 5(b), thus, show that both the temperature difference $T_h - T_c$ and the laser beam can be used to determine the effective thermal conductivity of a sample nanowire bonded to a VO_2 one.

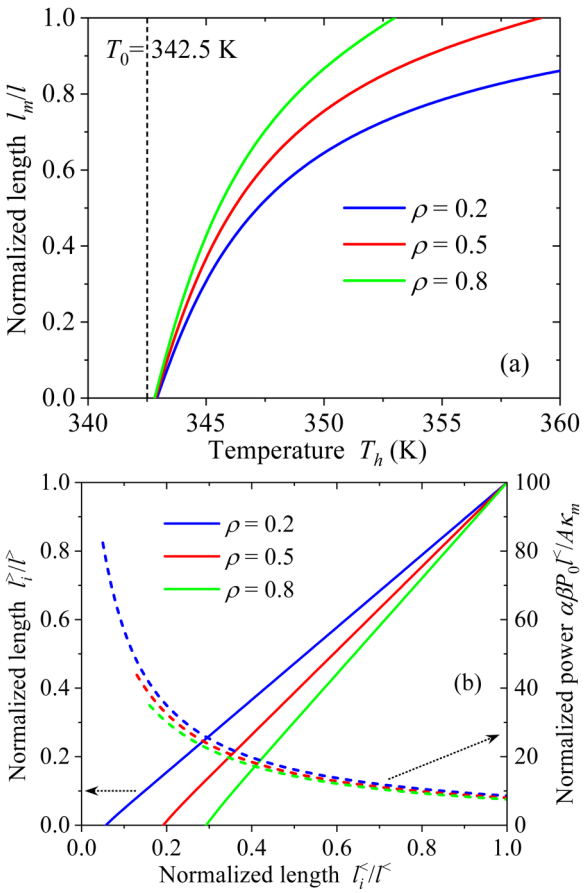

FIG. 5. (a) Temperature evolution of the normalized length of the metallic domain of a VO_2 nanowire in contact with a sample nanowire, as shown in Fig. 1(b). (b) Normalized length $l_i^>/l^>$ of the right insulating domain of a VO_2 nanowire as a function of its left counterpart $l_i^</l^<$ for the configuration shown in Fig. 1(d). The nonlinear relation between the absorbed power and $l_i^</l^<$ is also shown in (b). Calculations were done for $T_c = 335$ K, $R_h = R_m/10$, $l^< = l^>$, and three representative values of $\rho = (R + R_s + R_c)/R_m$.

IV. CONCLUSIONS

Based on the strong contrast of the thermal and optical properties of VO_2 through its metal–insulator transition, we have developed a theoretical methodology to determine the thermal conductivity of a single nanowire bonded to a VO_2 one and excited with either a temperature difference or a laser beam. Considering the non-linear heat conduction along a VO_2 nanowire, explicit expressions for the heat flux, temperature profile, and position of the metal/insulator domain interface have been derived and analyzed. For both thermal excitations, we have demonstrated that the metallic and insulating domains' lengths are quite sensitive to the thermal conductivity of the sample nanowire, and therefore, its optical observation could be used to determine this latter thermal property. Taking into account that the metal–insulator transition of VO_2 can be tuned via doping, the proposed methodology could be applied in a wide interval of temperatures and can be extended to the time or frequency domains to perform the thermal characterization of nanowires.

AUTHOR DECLARATIONS

Conflict of Interest

The authors have no conflicts to disclose.

Author Contributions

Jose Ordonez-Miranda: Conceptualization (equal); Data curation (equal); Formal analysis (equal); Investigation (equal); Methodology (equal); Resources (equal); Software (equal); Validation (equal); Visualization (equal); Writing – original draft (equal); Writing – review & editing (equal). **Laurent Belliard:** Data curation (equal); Formal analysis (equal); Validation (equal); Writing – review & editing (equal).

DATA AVAILABILITY

The data that support the findings of this study are available from the corresponding author upon reasonable request.

REFERENCES

[1]M. M. Qazilbash, M. Brehm, B. G. Chae, P. C. Ho, G. O. Andreev, B. J. Kim, S. J. Yun, A. V. Balatsky, M. B. Maple, F. Keilmann, H. T. Kim, and D. N. Basov, "Mott transition in VO_2 revealed by infrared spectroscopy and nano-imaging," Science **318**, 1750 (2007).
[2]M. M. Qazilbash, M. Brehm, G. O. Andreev, A. Frenzel, P. C. Ho, B. G. Chae, B. J. Kim, S. J. Yun, H. T. Kim, A. V. Balatsky, O. G. Shpyrko, M. B. Maple, F. Keilmann, and D. N. Basov, "Infrared spectroscopy and nano-imaging of the insulator-to-metal transition in vanadium dioxide," Phys. Rev. B **79**, 075107 (2009).
[3]J. Wu, Q. Gu, B. S. Guiton, N. P. de Leon, L. Ouyang, and H. Park, "Strain-induced self organization of metal-insulator domains in single-crystalline VO_2 nanobeams," Nano Lett. **6**, 2313 (2006).
[4]J. Ordonez-Miranda, Y. Ezzahri, K. Joulain, J. Drevillon, and J. J. Alvarado-Gil, "Modeling of the electrical conductivity, thermal conductivity, and specific heat capacity of VO_2," Phys. Rev. B **98**, 075144 (2018).
[5]D.-W. Oh, C. Ko, S. Ramanathan, and D. G. Cahill, "Thermal conductivity and dynamic heat capacity across the metal-insulator transition in thin film VO_2," Appl. Phys. Lett. **96**, 151906 (2010).
[6]J. Ordonez-Miranda, J. M. Hill, K. Joulain, Y. Ezzahri, and J. Drevillon, "Conductive thermal diode based on the thermal hysteresis of VO_2 and nitinol," J. Appl. Phys. **123**, 085102 (2018).
[7]C. L. Gomez-Heredia, J. A. Ramirez-Rincon, J. Ordonez-Miranda, O. Ares, J. J. Alvarado-Gil, C. Champeaux, F. Dumas-Bouchiat, Y. Ezzahri, and K. Joulain, "Thermal hysteresis measurement of the VO_2 emissivity and its application in thermal rectification," Sci. Rep. **8**, 8479 (2018).
[8]J. A. Ramirez-Rincon, C. L. Gomez-Heredia, A. Corvisier, J. Ordonez-Miranda, T. Girardeau, F. Paumier, C. Champeaux, F. Dumas-Bouchiat, Y. Ezzahri, K. Joulain, O. Ares, and J. J. Alvarado-Gil, "Thermal hysteresis measurement of the VO_2 dielectric function for its metal-insulator transition by visible-IR ellipsometry," J. Appl. Phys. **124**, 195102 (2018).
[9]P. Ben-Abdallah and S. A. Biehs, "Phase-change radiative thermal diode," Appl. Phys. Lett. **103**, 191907 (2013).
[10]P. Ben-Abdallah and S. A. Biehs, "Near-field thermal transistor," Phys. Rev. Lett. **112**, 044301 (2014).

[11]K. Joulain, Y. Ezzahri, J. Drevillon, and P. Ben-Abdallah, "Modulation and amplification of radiative far field heat transfer: Towards a simple radiative thermal transistor," Appl. Phys. Lett. **106**, 133505 (2015).
[12]H. Prod'homme, J. Ordonez-Miranda, Y. Ezzahri, J. Drevillon, and K. Joulain, "Optimized thermal amplification in a radiative transistor," J. Appl. Phys. **119**, 194502 (2016).
[13]J. Ordonez-Miranda, Y. Ezzahri, J. Drevillon, and K. Joulain, "Dynamical heat transport amplification in a far-field thermal transistor of VO_2 excited with a laser of modulated intensity," J. Appl. Phys. **119**, 203105 (2016).
[14]I. Forero-Sandoval, J. Chan-Espinoza, J. Ordonez-Miranda, J. Alvarado-Gil, F. Dumas-Bouchiat, C. Champeaux, K. Joulain, Y. Ezzahri, J. Drevillon, C. Gomez-Heredia, and J. Ramirez-Rincon, "VO_2 substrate effect on the thermal rectification of a far-field radiative diode," Phys. Rev. Appl. **14**, 034023 (2020).
[15]Y. Li, Y. Dang, S. Zhang, X. Li, Y. Jin, P. Ben-Abdallah, J. Xu, and Y. Ma, "Radiative thermal transistor," Phys. Rev. Appl. **20**, 024061 (2023).
[16]J. W. Lim, A. Majumder, R. Mittapally, A.-R. Gutierrez, Y. Luan, E. Meyhofer, and P. Reddy, "A nanoscale photonic thermal transistor for sub-second heat flow switching," Nat. Commun. **15**, 5584 (2024).
[17]P. Ben-Abdallah, "Thermal memristor and neuromorphic networks for manipulating heat flow," AIP Adv. **7**, 065002 (2017).
[18]J. Ordonez-Miranda, Y. Ezzahri, J. A. Tiburcio-Moreno, K. Joulain, and J. Drevillon, "Radiative thermal memristor," Phys. Rev. Lett. **123**, 025901 (2019).
[19]F. Yang, M. P. Gordon, and J. J. Urban, "Theoretical framework of the thermal memristor via a solid-state phase change material," J. Appl. Phys. **125**, 025109 (2019).
[20]G. Li, Z. Wang, Y. Chen, J.-C. Jeon, and S. S. P. Parkin, "Computational elements based on coupled VO_2 oscillators via tunable thermal triggering," Nat. Commun. **15**, 5820 (2024).
[21]X. Wu, Y. Tao, L. Dong, Z. Wang, and Z. Hu, "Preparation of VO_2 nanowires and their electric characterization," Mater. Res. Bull. **40**, 315 (2005).
[22]C. Cheng, D. Fu, K. Liu, H. Guo, S. Xu, S.-G. Ryu, O. Ho, J. Zhou, W. Fan, W. Bao, M. Salmeron, N. Wang, C. P. Grigoropoulos, and J. Wu, "Directly metering light absorption and heat transfer in single nanowires using metal–insulator transition in VO_2," Adv. Opt. Mater. **3**, 336 (2015).
[23]A. C. Jones, S. Berweger, J. Wei, D. Cobden, and M. B. Raschke, "Nano-optical investigations of the metal-insulator phase behavior of individual VO_2 microcrystals," Nano Lett. **10**, 1574 (2010).
[24]C. Cheng, K. Liu, B. Xiang, J. Suh, and J. Wu, "Ultra-long, free-standing, single-crystalline vanadium dioxide micro/nanowires grown by simple thermal evaporation," Appl. Phys. Lett. **100**, 103111 (2012).
[25]K.-N. Lee, S.-W. Jung, K.-S. Shin, W.-H. Kim, M.-H. Lee, and W.-K. Seong, "Fabrication of suspended silicon nanowire arrays," Small **4**, 642 (2008).
[26]L. Shi, D. Li, C. Yu, W. Jang, D. Kim, Z. Yao, P. Kim, and A. Majumdar, "Measuring thermal and thermoelectric properties of one-dimensional nanostructures using a microfabricated device," J. Heat Transf. **125**, 881 (2003).
[27]M. Rocci, V. Demontis, D. Prete, D. Ercolani, L. Sorba, F. Beltram, G. Pennelli, S. Roddaro, and F. Rossella, "Suspended InAs nanowire-based devices for thermal conductivity measurement using the 3ω method," J. Mater. Eng. Perform. **27**, 6299 (2018).
[28]L. Belliard, T. W. Cornelius, B. Perrin, N. Kacemi, L. Becerra, O. Thomas, M. Eugenia Toimil-Molares, and M. Cassinelli, "Vibrational response of free standing copper nanowire through transient reflectivity microscopy," J. Appl. Phys. **114**, 193509 (2013).
[29]M. Aziz, D. Christopher Hudson, and S. Russo, "Molybdenum-rhenium superconducting suspended nanostructures," Appl. Phys. Lett. **104**, 233102 (2014).
[30]C. Cheng, W. Fan, J. Cao, S.-G. Ryu, J. Ji, C. P. Grigoropoulos, and J. Wu, "Heat transfer across the interface between nanoscale solids and gas," ACS Nano **5**, 10102 (2011).